J. Astrophys. Astr. (2020) 41:47
https://doi.org/10.1007/s12036-020-09670-7
© Indian Academy of Sciences

i-Process nucleosynthesis: Observational evidences from CEMP stars

PARTHA PRATIM GOSWAMI* and ARUNA GOSWAMI*

Indian Institute of Astrophysics, Sarjapur Road, Koramangala, Bengaluru 560034, India.
*Corresponding author. E-mail: partha.pg@iiap.res.in; aruna@iiap.res.in

MS received 30 August 2020; accepted 5 October 2020

Abstract. The surface chemical compositions of a large fraction of carbon-enhanced metal-poor (CEMP) stars, the so-called CEMP-r/s stars, are known to exhibit enhancement of both s-process and r-process elements. For these stars, the heavy-element abundances cannot be explained either by s-process or r-process nucleosynthesis alone, as the production sites of s-process and r-process elements are very different, and these two processes produce distinct abundance patterns. Thus, the observational evidence of the double enhancement seen in CEMP-r/s stars remains a puzzle as far as the origin of the elements is concerned. In this work, we have critically analysed the observed abundances of heavy elements in a sample of eight CEMP-r/s stars from the literature to trace the origin of the observed double enhancement. Towards this, we have conducted a parametric-model-based analysis to delineate the contributions of s-process and r-process nucleosynthesis to the observed elemental abundances. We have further examined if the i-process (intermediate-process) nucleosynthesis that occurs at high neutron density (n $\sim 10^{15}$ cm^{-3}) produced during proton ingestion from a H-rich envelope to the intershell region of an AGB star, which is capable of producing both r-process and s-process elements in a single stellar site, could explain the observed abundance patterns of the sample stars. Our analysis shows that the observed abundance patterns of the selected sample of CEMP-r/s stars could be fairly well reproduced using the i-process model yields.

Keywords. Stars—nucleosynthesis—i-process.

1. Introduction

Most of the elements heavier than iron are produced in stars by slow (s) and rapid (r) neutron-capture nucleosynthesis processes. In the slow-neutron-capture process (s-process) the timescale for neutron capture is usually much longer than that for the β-decay of unstable nuclei along the s-process path, whereas in the rapid-neutron-capture process (r-process) the timescale for neutron capture is much shorter than the β-decay process. While the s-process operates with a neutron density of 10^{6-10} cm^{-3} (Busso *et al.* 1999) in the inter-pulse phases of low-mass and intermediate-mass AGB stars (Gallino *et al.* 1998), the r-process requires very high temperatures and neutron fluxes (n $> 10^{20}$ cm^{-3}) and is expected to occur during supernova explosions and neutron star mergers (Thielemann *et al.* 2011; Wehmeyer *et al.* 2015). These two processes are characterized by distinct elemental abundance patterns. A large fraction of carbon-enhanced metal-poor (CEMP) stars are known to exhibit enhancement of s-process elements (CEMP-s stars) in surface chemical composition, a few exhibit enhancement in r-process elements (CEMP-r stars), a sizeable fraction show enhancement of both s-process and r-process elements (CEMP-r/s stars), and a few stars do not show enhancement of heavy elements (CEMP-no stars) (Beers & Christlieb 2005; Aoki

This article is part of the Topical Collection: Chemical elements in the Universe: Origin and evolution.

Published online: 17 December 2020

et al. 2007). In general, CEMP stars are characterized by [Fe/H][1] < -1.0 and [C/Fe] > 1.0, and barium and europium are considered as the representative elements of s-process and r-process respectively (Beers & Christlieb 2005). Chemical composition studies on CEMP-r/s stars have revealed that the observed heavy-element abundances cannot be explained by either s-process or r-process nucleosynthesis alone (Aoki *et al.* 2015, 2017). To explain the abundance pattern of the CEMP-r/s stars different formation scenarios have been proposed, involving different production sites for the s-process and r-process elements (Jonsell *et al.* 2006; Lugaro *et al.* 2009; Abate *et al.* 2016). All these scenarios are, however, not free from certain uncertainties, either in explaining the observed frequency of these stars, or the observed abundance patterns. An alternative process called 'i-process (intermediate process) nucleosynthesis' has recently been suggested as a possible production mechanism for CEMP-r/s stars (Dardelet *et al.* 2014; Hampel *et al.* 2016, 2019). Although it has been known for long (Cowan & Rose 1977) that proton ingestion from the convective envelope to the inter-shell region of AGB stars can produce high neutron flux which can initiate i-process nucleosynthesis, it is only very recently that it has been explored to understand the observed abundance patterns of CEMP-r/s stars on the basis of i-process (Dardelet *et al.* 2014; Hampel *et al.* 2016, 2019). Different sites have been proposed for the proton-ingestion episodes (PIE), such as core-helium flash (Fujimoto *et al.* 1990; Lugaro *et al.* 2009, the most massive AGB stars (Jones *et al.* 2016), and the super AGB stars (Doherty *et al.* 2015). However, the physical conditions under which proton ingestion can take place still remain a matter of debate. Many details regarding the site of the i-process nucleosynthesis that operates with neutron densities $n \sim 10^{15}$ cm^{-3} also remain poorly understood.

In this work, to understand the origin of the abundance patterns of heavy elements in CEMP-r/s stars, we have chosen a sample of eight stars reported to be CEMP-r/s stars by various researchers (Goswami *et al.* 2006; Goswami & Aoki 2010; Allen *et al.* 2012; Hansen *et al.* 2019; Purandardas *et al.* 2019) based on their estimates of abundances and abundance ratios of heavy elements for these stars. We have performed a parametric-model-based study to delineate the contributions of s-process and r-process to the observed heavy-element abundances. With reference to the sample stars, we have discussed and examined different formation scenarios to understand the processes responsible for the double enhancement seen in these stars. We find that using i-process model yields we could reproduce the observed abundance patterns of heavy elements of the sample of CEMP-r/s stars chosen for this study.

In Section 2, we have discussed in brief the sample of CEMP-r/s stars taken from the literature for this study. Section 3 discusses the procedure and results of the parametric-model-based study. In Section 4.1, different formation scenarios have been discussed in the context of the abundance pattern observed in the sample stars. Section 4.2 discusses the i-process models and results of the comparison of the model predictions with the observed heavy-element abundances of our sample stars. We report our conclusions in Section 5.

2. Sample of CEMP-r/s stars: CD−28 1082, CS 29503−010, CS 29528−028, HD 209621, HE 0002−1037, HE 0059−6540, HE 0151−6007, HE 1305+0007

The objects were selected following CEMP stars criteria (i.e. [Fe/H] < -1, and [C/Fe] > 0.7). In our sample, the CEMP-r/s stars have metallicity in the range $-1.70 <$ [Fe/H] < -2.70. In Purandardas *et al.* (2019) we have derived the atmospheric parameters and, for the first time, estimated the elemental abundances of CD−28 1082. The object was found to be a CEMP-r/s star with [Ba/Fe] = 2.09, [Eu/Fe] = 2.07 and [Ba/Eu] = 0.02, with ^{12}C/^{13}C ratio $\sim$ 16. The objects HE 0002−1037, HE 0059−6540 and HE 0151−6007 have been reported to be CEMP-r/s by Hansen *et al.* (2019). These three objects exhibit abundances of Ba and Eu in the ranges $1.7 <$ [Ba/Fe] < 2.3 and $1.5 <$ [Eu/Fe] < 2.3, with [Ba/Eu] < 0.5 in each case. Hansen *et al.* (2019) estimated the ^{12}C/^{13}C ratio to be 24 and 1 for the objects HE 0002−1037 and HE 0059−6540 respectively. The kinematic analysis shows that all these four sample stars belong to the inner halo population in the Galaxy. Allen *et al.* (2012) classified the objects CS 29503−010 and CS 29528−028 to be CEMP-r/s stars with [Ba/Fe] = 1.81 and 2.49 and [Eu/Fe] = 1.69 and 2.16 respectively on the basis of their analysis. Elemental abundances of two CEMP-r/s stars HE 1305 + 0007 and

[1]**Notation:** [A/B] = $\log(N_A/N_B)_* - \log(N_A/N_B)_\odot$, where N_A and N_B are number densities of elements A and B respectively.

Table 1. Atmospheric parameters of the sample stars.

Star name	T_{eff} (K)	log g	ζ (km s^{-1})	[Fe/H]
CD−28 1082[a]	5200	1.90	1.42	−2.45
CS 29503−010[b]	6050	3.66	1.60	−1.70
CS 29528−028[b]	7100	4.27	1.20	−2.15
HD 209621[c]	4500	2.00	2.00	−1.93
HE 0002−1037[d]	5010	2.00	1.80	−2.40
HE 0059−6540[d]	5040	2.10	1.80	−2.20
HE 0151−6007[d]	4350	1.00	2.10	−2.70
HE 1305+0007[e]	4750	2.00	2.00	−2.01

(*a*) Purandardas *et al.* (2019), (*b*) Allen *et al.* (2012), (*c*) Goswami and Aoki (2010), (*d*) Hansen *et al.* (2019), (*e*) Goswami *et al.* (2006).

HD 209621 have been taken from Goswami *et al.* (2006) and Goswami and Aoki (2010) respectively. Tsuji *et al.* (1991) and Goswami *et al.* (2006) estimated $^{12}C/^{13}C$ ratio to be $\sim$ 10 for both HD 209621 and HE 1305 + 0007.

The atmospheric parameters of the sample stars are presented in Table 1. The abundance ratios of neutron-capture elements and carbon with respect to Fe are presented in Table 2.

3. Parametric-model-based study

To understand the origin of the observed abundances in the sample stars, it is important to identify the contribution of the dominant neutron-capture process. Following the procedure described in Goswami *et al.* (2010) and references therein, we have performed a parametric-model-based study to trace the contributions of s-process and r-process nucleosynthesis to the observed abundances of the heavy elements. We have normalized the Solar s-process and r-process isotopic abundances of the stellar models of Arlandini *et al.* (1999) to the barium abundances of the corresponding CEMP-r/s stars. The observed elemental abundances of the sample stars are then fitted with the parametric model function $\log \epsilon_i = C_s N_{is} + C_r N_{ir}$, where N_{is} indicates the normalized abundance from s-process, N_{ir} indicates the normalized abundance from r-process, C_s indicates the component coefficient that corresponds to contributions from the s-process, and C_r indicates the component coefficient that corresponds to contributions from the r-process.

The best fitting coefficients and χ^2 values are presented in Table 3. Figure 1 shows the best model fits with the observed abundances of the sample stars. Goswami and Aoki (2010) performed a parametric-model-based analysis of the heavy-element

Table 2. Abundance ratios of neutron-capture elements of the sample stars.

Star name	[Fe/H]	[C/Fe]	[Sr/Fe]	[Y/Fe]	[Zr/Fe]	[Ba/Fe]	Ref.
CD−28 1082	− 2.45	2.19	1.44	1.61	–	2.09	*a*
CS 29503−010	− 1.70	1.65	1.13	1.09	1.26	1.81	*b*
CS 29528−028	− 2.15	2.76	1.72	1.99	2.17	2.49	*b*
HD 209621	− 1.93	1.25	1.02	0.36	1.80	1.70	*c*
HE 0002−1037	− 2.40	1.90	<1.00	0.40	–	2.00	*d*
HE 0059−6540	− 2.20	1.40	1.20	0.40	–	1.70	*d*
HE 0151−6007	− 2.70	1.70	1.10	0.80	–	2.30	*d*
HE 1305+0007	− 2.01	1.84	0.86	0.73	2.09	2.32	*e*

Star name	[La/Fe]	[Ce/Fe]	[Pr/Fe]	[Nd/Fe]	[Sm/Fe]	[Eu/Fe]	Ref.
CD−28 1082	1.55	1.97	2.30	1.99	2.29	2.07	*a*
CS 29503−010	2.16	2.05	–	2.31	2.34	1.69	*b*
CS 29528−028	2.21	2.47	–	2.54	–	2.16	*b*
HD 209621	2.41	2.04	2.16	1.87	1.46	1.35	*c*
HE 0002−1037	2.00	1.70	2.10	2.10	–	1.70	*d*
HE 0059−6540	1.60	1.40	1.40	1.70	–	1.50	*d*
HE 0151−6007	2.50	2.40	2.60	2.60	–	2.30	*d*
HE 1305+0007	2.56	2.53	2.38	2.59	2.60	1.97	*e*

References: (*a*) Purandardas *et al.* (2019), (*b*) Allen *et al.* (2012), (*c*) Goswami and Aoki (2010), (*d*) Hansen *et al.* (2019), (*e*) Goswami *et al.* (2006).

Table 3. Best-fit coefficients and χ^2 for the parametric model function $log\epsilon_i = C_s N_{is} + C_r N_{ir}$.

Star name	C_s	C_r	χ^2
CD−28 1082	0.48	0.52	4.97
CS 29503−010	0.37	0.63	6.76
CS 29528−028	0.48	0.52	1.06
HD 209621[a]	0.57	0.52	1.80
HE 0002−1037	0.41	0.59	10.73
HE 0059−6540	0.47	0.53	7.83
HE 0151−6007	0.21	0.79	11.91
HE 1305+0007[a]	0.47	0.53	1.07

(*a*) Goswami and Aoki (2010).

abundances observed in HD 209621 and HE 1305+0007 and concluded that similar contributions of both s-process and r-process are required to explain the abundance pattern of the stars (see Figure 5 of Goswami & Aoki (2010)). We have confirmed these results based on our analysis.

4. Discussion

4.1 *Different scenarios for formation of CEMP-r/s stars*

To explain the peculiar abundance pattern of CEMP-r/s stars, researchers have proposed several formation scenarios (Jonsell *et al.* 2006; Lugaro *et al.* 2009; Abate *et al.* 2016). Here, we have discussed briefly some of the scenarios that are considered relevant for the sample of CEMP-r/s stars under this study.

(i) Radiative levitation, where the partially ionized heavy elements having large photon absorption cross-sections are pushed outwards by radiative pressure, could be a possible scenario for the observed over-abundance of heavy elements in CEMP-r/s stars. However, the simulations of Richard *et al.* (2002) and Matrozis and Stancliffe (2016) have shown that the process of radiative levitation can occur in the hot stars in their main-sequence and main-sequence turn-off phases of evolution due to their thin convective envelopes. The sample stars in this study are low-temperature objects with temperature in the range 4350 K − 7100 K, and the radiative levitation scenario may not be applicable to explain the observed abundance pattern of these stars. This scenario has also been discussed at length by Cohen *et al.* (2003), Jonsell *et al.* (2006) and Abate *et al.* (2016) and rejected as a possible mechanism for formation of CEMP-r/s stars.

(ii) There are two scenarios where the enhancement of r-process elements in the CEMP-r/s stars is attributed to the r-process-material-enriched ISM from which the star is formed. In these scenarios, it is proposed that the enrichment of s-process elements is either due to self-contamination in its AGB phase (Hill *et al.* 2000; Cohen *et al.* 2003; Jonsell *et al.* 2006) or AGB pollution in a binary system (Hill *et al.* 2000; Cohen *et al.* 2003; Ivans *et al.* 2005; Jonsell *et al.* 2006; Bisterzo *et al.* 2011).

In the self-contamination scenario, the star needs to pass through the AGB phase of evolution to undergo s-process nucleosynthesis. However, the evolutionary stage of CEMP-r/s stars studied so far reveals that they have not yet passed through the red-giant-branch phase to produce the s-process

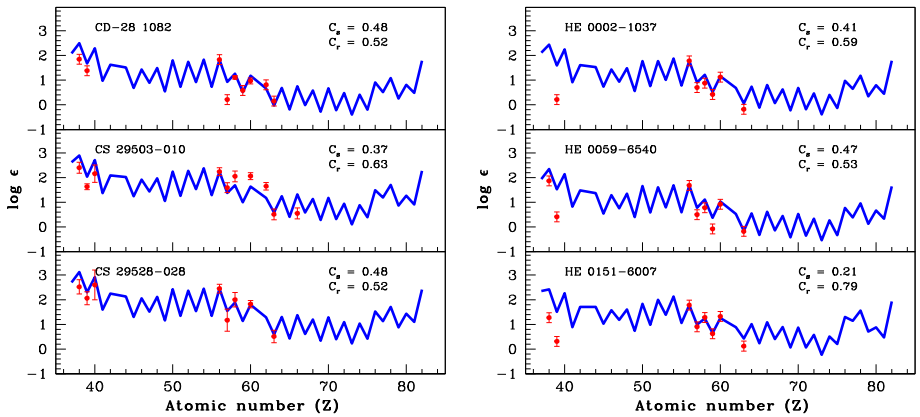

Figure 1. Solid curve represents the best fit for the parametric-model function $log\epsilon_i = C_s N_{is} + C_r N_{ir}$, where N_{is} and N_{ir} represent the abundances due to s-process and r-process respectively (isotopic abundances from the stellar model of Arlandini *et al.* (1999) are normalized to the Ba abundances of the corresponding stars). The points with error bars indicate the observed abundances.

elements. For this reason, this scenario had been rejected by many researchers (Jonsell *et al.* 2006; Abate *et al.* 2016). Two objects in our sample, CS 29503−010 and CS 29528−028, exhibit log g values ($\sim$ 4.0), similar to that of dwarfs or subgiants. The rest of the stars show low values ($\sim$ 1 − 24) of $^{12}C/^{13}C$ implying the extrinsic nature of heavy elements and carbon in these stars. Thus, this scenario is not applicable to our sample stars.

In another scenario, the primary, being more massive than the other in the binary system formed from the r-process-material-enriched ISM, evolves faster and proceeds through the AGB phase, producing s-process elements along with carbon. The mass-transfer episodes in the AGB phase then make the secondary star enriched in s-process elements. Considering this scenario of pre-enrichment of the binary system with r-process elements from the r-rich molecular cloud, Bisterzo *et al.* (2011, 2012), tried to reproduce the observed [hs/ls] in the CEMP-r/s stars. Although they claimed to be successful in doing so (compatible within error bars), there are still some arguments against this scenario. It is found that the abundances of Ba and Eu are correlated in CEMP-r/s stars and the AGB models cannot explain this correlation in case of independent enrichment of s-process and r-process elements (Abate *et al.* 2016). Also, the large fraction of CEMP-r/s stars among the CEMP-s stars cannot be explained by this scenario (Jonsell *et al.* 2006; Lugaro *et al.* 2009).

(iii) This scenario explains how a star can acquire s-process and r-process elements in a triple-star system. The most massive one among the three stars evolves the fastest, and supernova explosion of this star makes the other two stars r-rich. Then, the more massive one among the other two stars evolves through the AGB phase and produces s-process elements along with carbon. AGB mass transfer from this star makes the tertiary a CEMP-r/s star (Cohen *et al.* 2003; Jonsell *et al.* 2006). However, it seems very unlikely that after the supernova explosion the triple system survives for further mass transfer. Abate *et al.* (2016) could not reproduce the observed frequency of CEMP-r/s stars among CEMP-s stars and hence dismissed this scenario.

(iv) There are two proposed scenarios that considered binary systems where the s-process elements in the CEMP-r/s star are assumed to come from the primary through its AGB phase, and r-process elements are attributed to either a type 1.5 supernova (Zijlstra 2004; Jonsell *et al.* 2006) or an accretion-induced collapse (AIC) (Qian & Wasserburg 2003; Cohen *et al.* 2003).

In the first scenario, the primary star, being more massive than the other in the binary system, evolves through the AGB phase. During the AGB phase, the star produces and transfers s-process-rich material to the companion. Then, the AGB star may explode as a type 1.5 supernova and pollute the companion with r-process elements, making the secondary a CEMP-r/s star. Iben and Renzini (1983) gave the name 'type 1.5 supernovae' to the process when the degenerate cores of high-mass AGB stars, due to low mass-loss efficiency at low metallicity, remain as massive as to reach the Chandrasekhar mass limit and explode (Zijlstra 2004). However, Nomoto *et al.* (1976), Iben and Renzini (1983) and Lau *et al.* (2008) stated that type 1.5 supernova can destroy the primary star and hence disrupt the binary system. As most of the CEMP-r/s stars have been reported to be found in binary systems (Lucatello *et al.* 2005; Abate *et al.* 2016) rejected this scenario.

In the other scenario, after transferring the AGB-processed material (s-process elements) to the companion star, the primary star becomes a white dwarf. Then, as time progresses, the secondary star evolves to the giant branch and transfers material back to the white dwarf. This mass transfer may trigger an accretion-induced collapse (AIC) and hence pollute the secondary star with r-process material (Qian & Wasserburg 2003; Cohen *et al.* 2003). This scenario demands that the secondary star remain in the giant branch to fill the Roche lobe for the second phase of mass transfer. This scenario may be rejected as the observed CEMP-r/s stars are not always giants (Lugaro *et al.* 2009). In many cases, these stars are seen in the main sequence turn-off, making the accretion process difficult. (Abate *et al.* 2016) stated that the three phases of mass transfer work properly only if the orbital separation of the binary system is narrow, but the observed frequency of CEMP-r/s stars could not be reproduced even by considering a narrow separation. Also, there are uncertainties regarding the efficiency of AIC to produce enough r-process elements to match the observed abundances of heavy elements in CEMP-r/s stars (Qian & Woosley 1996; Qian & Wasserburg 2003).

(v) A formation scenario named 'intermediate neutron-capture process or i-process', similar to the formation scenarios for CH, Ba and CEMP-s stars, has been proposed recently to explain the abundances of CEMP-r/s stars. This scenario considers a binary system where one star is slightly more massive than the other. The more massive star evolves faster and passes through the AGB phase, polluting the

companion with AGB-processed material. The difference of this scenario from the s-process-enrichment scenarios is that in this scenario a neutron density (n $\sim 10^{15}$ cm^{-3}), which is intermediate to the neutron densities of both s-process and r-process, can produce the double enhancement seen in CEMP-r/s stars (Cowan and Rose 1977; Dardelet *et al.* 2014; Hampel *et al.* 2016). Cowan and Rose (1977), for the first-time, suggested the possibility of occurrence of i-process in AGB stars. They found that significantly high neutron density can be achieved by mixing hydrogen-rich material into the intershell region of AGB stars. Using i-process models (Dardelet *et al.* 2014) and Hampel *et al.* (2016) have successfully reproduced the abundance distribution of a number of well-known CEMP-r/s stars.

4.2 *Comparison of the abundance pattern of the sample stars with i-process model*

Dardelet *et al.* (2014) and Hampel *et al.* (2016) calculated i-process-model yields with slightly different approaches, but both groups could successfully reproduce the observed abundance pattern of CEMP-r/s stars. Single-zone nuclear network calculations were used in both the studies. Assuming proton ingestion from the H-rich envelope by the He-pulse-driven convective zone (PDCZ) to be responsible for the generation of higher neutron densities ($n \sim 10^{15}$cm^{-3}), Dardelet *et al.* (2014) used a constant combined mass fraction of C+H (= 0.7) in their simulations. They considered the termination time of the i-process as a free parameter for their calculations. On the other hand, Hampel *et al.* (2016) calculated the yields of the neutron-capture nucleosynthesis, assuming the nucleosynthesis to operate in the intershell region of an AGB star, at different constant neutron densities starting from n $\sim 10^7$ cm^{-3} to 10^{15} cm^{-3}. Dardelet *et al.* (2014) assumed the temperature and density for the He PDCZ to be 2.0×10^8 K and 10^4 g cm^{-3} respectively. These physical input parameters are chosen so as to prevent proton capture by ^{13}N and allow the ^{13}C(α, n)^{16}O reaction for neutron release. As a test, Hampel *et al.* (2016) tried to calculate the yields with a range of temperatures (1×10^8 K to 2.2×10^8 K) and densities (800 g cm^{-3} to 3200 g cm^{-3}), but did not see significant changes in the results. However, for the final simulations they adopted the parameters (T = 1.5×10^8 K and ρ = 1600 g cm^{-3}) of the intershell region of a low-metallicity (z = 10^{-4}), low-mass (M = 1 M$_\odot$) AGB star (Stancliffe *et al.* 2011). As initial abundances of the He PDCZ, Dardelet *et al.* (2014) considered solar abundances (except C and O), scaled down to z = 10^{-3}. The abundances of C and O are taken to be X(^{12}C)=0.5 and X(^{16}O)=0.05, which are typical abundances for the He PDCZ. Hampel *et al.* (2016) adopted the constituents of the intershell region from Abate *et al.* (2015). A high neutron exposure of $\tau \sim 495$ mb^{-1} is ensured by adjusting the run times of the models. Due to such high neutron exposures, the abundance pattern of heavy elements and the seed nuclei comes to an equilibrium, which makes the element-to-element ratio a function of constant neutron density.

In the model of Dardelet *et al.* (2014), almost all of the ^{12}C isotopes get transformed into ^{13}N during the first second of run-time. Then, in 9.97 minutes, ^{13}N decays to form ^{13}C, which captures α to release neutrons with high neutron densities through the reaction ^{13}C(α, n)^{16}O. The neutron exposure (τ) increases with time, reaching up to $10 - 50$ mb^{-1}, and subsequently the heavier elements are produced. This model could successfully reproduce the observed abundance pattern of three CEMP-r/s stars. On the other hand, Hampel *et al.* (2016) noticed that, when the neutron exposure was kept switched on, for lower neutron densities (n $\sim 10^7$ cm^{-3}) typical s-process abundance pattern is produced, with stable peaks of ls (Sr, Y, Zr) and hs (Ba, La, Ce) elements. But with higher neutron densities (n = $10^{12} - 10^{15}$ cm^{-3}), both ls and hs element peaks shift to lighter elements. In particular, a peak at ^{135}I is formed due to the i-process neutron densities. Then, the neutron exposure is turned off for t = 10 Myr. During this time, it is noticed that unstable isotopes decay to produce stable isotopes at ls and hs peaks. The decay of ^{135}I produces ^{135}Ba. With increasing neutron densities, abundances of Ba and Eu are found to increase. This is how the abundance pattern gets modified due to i-process. Using this i-process model, Hampel *et al.* (2016) could successfully reproduce the observed abundance pattern of twenty CEMP-r/s stars, including the three previously reproduced by the i-process model of Dardelet *et al.* (2014).

We have used the model predictions ([X/Fe]) for neutron densities ranging from n $\sim 10^9$ to n $\sim 10^{15}$ cm^{-3} (Hampel *et al.* 2016), and compared them with the elemental abundance pattern of our sample of CEMP-r/s stars. To examine whether the i-process models could reproduce the observed abundances of the sample stars we have followed the procedure

discussed in Hampel *et al.* (2016) and used the equation

$$X = X_i \times (1 - d) + X_\odot \times d, \quad (1)$$

where X_i is the model yield, $X_\odot$ is solar-scaled abundance, and d is a dilution factor.

Table 4 presents the values of the fit parameters neutron density, 'd' and 'χ^2' for each star. The best-fit neutron density for each of the sample stars is chosen for which we got the minimum value of 'χ^2'. The best-fit models with appropriate neutron densities and corresponding dilution factors are shown in Figure 2. We have found that i-process models with neutron densities of n $\sim$ 10^{12} cm^{-3} to 10^{14} cm^{-3} closely fit the observed abundances of the sample stars. We have obtained a neutron density of n $\sim$ 10^{14} cm^{-3} for the star HE 1305+0007, which is same as that reported by Hampel *et al.* (2016) for the object. Hampel *et al.* (2019) tried to understand i-process nucleosynthesis through the abundances of Pb in CEMP-r/s stars. In their i-process models (Hampel *et al.* 2019) considered neutron exposure (τ) as a free parameter along with dilution factor (d). Varying 'd' and 'τ' at different constant neutron densities, they could fit the observed abundances of HE 1305+0007 and HD 209621 with models with neutron densities n $\sim$ 10^{14} cm^{-3} and 10^{13} cm^{-3} respectively. We too got the best fit at n $\sim$ 10^{13} cm^{-3} for the object HD 209621 taking only 'd' as a free parameter with constant 'τ'.

Table 4. Fit parameters of i-process model for the sample stars.

Star name	Neutron-density n (cm^{-3})	d	χ^2
CD−28 1082	10^{13}	0.9704	3.26
CS 29503−010	10^{13}	0.9745	2.74
CS 29528−028	10^{12}	0.9331	0.51
HD 209621	10^{13}	0.9798	3.52
HE 0002−1037	10^{14}	0.9766	1.71
HE 0059−6540	10^{13}	0.9908	2.34
HE 0151−6007	10^{14}	0.9274	2.06
HE 1305+0007	10^{14}	0.9262	2.62

5. Conclusions

In this study, we have examined if the currently available theoretical i-process stellar yields could adequately explain the enhancement in both s-process and r-process elements observed in a selected sample of CEMP-r/s stars. We have considered eight stars, of which the abundances of the heavy elements for three objects are taken from our previous studies (Goswami *et al.* 2006; Goswami & Aoki 2010; Purandardas *et al.* 2019) and those for the rest from other sources (Allen *et al.* 2012; Hansen *et al.* 2019).

With the help of a parametric-model-based study, we have estimated the contributions from s-process and r-process nucleosynthesis to the observed elemental abundances. It is found that similar contributions from both the processes are required to explain the observed abundance pattern of heavy elements in these stars.

With reference to the double enhancement seen in the sample stars, we have discussed different scenarios for formation of CEMP-r/s stars. The scenarios involving two stellar sites for the production of s-process and r-process elements are found to be not applicable to the sample of CEMP-r/s stars under this study. However, we have seen that the i-process

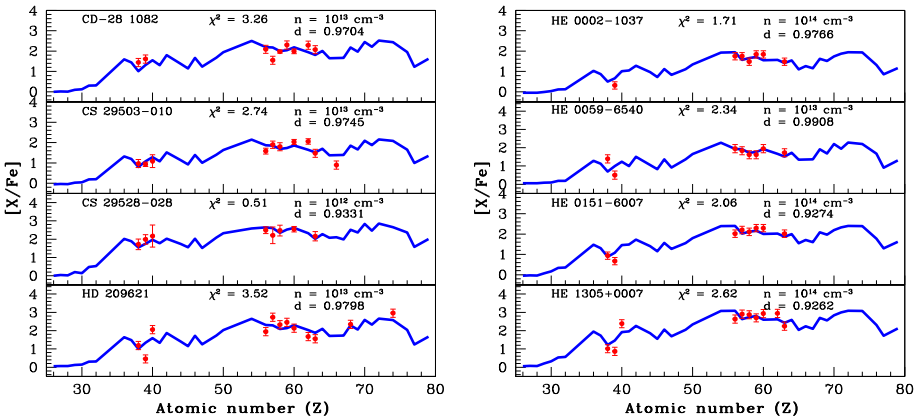

Figure 2. Best-fitting i-process model (solid blue curve) for the sample stars. The points with error bars indicate the observed abundances.

models of Hampel *et al.* (2016) can satisfactorily reproduce the observed overabundance of heavy elements in these stars. The i-process stellar yields required to fit the observed abundance patterns are found to correspond to neutron densities as high as 10^{12} cm^{-3} to 10^{14} cm^{-3}. The estimated low values of $^{12}C/^{13}C$ ratio observed in the stars agree well with i-process predictions, indicating the extrinsic nature of carbon and the heavy elements.

Acknowledgements

Funding from the DST SERB project EMR/2016/005283 is gratefully acknowledged. We are thankful to Melanie Hampel for providing us with the i-process yields in the form of number fractions. This work made use of the SIMBAD astronomical database, operated at CDS, Strasbourg, France, and NASA ADS, USA.

References

Abate C., Pols O. R., Karakas A. I., Izzard R. G. 2015, A&A, 576, A118
Abate C., Stancliffe R. J., Liu Z.-W. 2016, A&A, 587, A50
Allen D. M., Ryan S. G., Rossi S., Beers T. C., Tsangarides S. A. 2012, A&A, 548, A34
Aoki W., Beers T. C., Christlieb N., Norris J. E., Ryan S. G., Tsangarides, S. 2007, ApJ, 655, 492
Aoki M., Ishimaru Y., Aoki W., Wanajo S. 2017, ApJ, 837, 8
Aoki W., Suda T., Beers T. C., Honda S., 2015, AJ, 149, 39
Arlandini C., Käppeler F., Wisshak K., *et al*. 1999, ApJ, 525, 886
Beers T. C., Christlieb N. 2005, ARA&A, 43, 531
Bisterzo S., Gallino R., Straniero O., Cristallo S., Kappeler F. 2011, MNRAS, 418, 284
Bisterzo S., Gallino R., Straniero O., Cristallo S., Kappeler F. 2012, MNRAS, 422, 849
Busso M., Gallino R., Wasserburg G. J. 1999, ARA&A, 37, 239
Cohen J. G., Christlieb N., Qian Y.-Z., Wasserburg G. J. 2003, ApJ, 588, 1082
Cowan J. J., Rose W. K. 1977, ApJ, 212, 149
Dardelet L., Ritter C., Prado P., *et al*. 2014, in Proc. XIII Nuclei in the Cosmos Symp., ed. Z. Elekes, Z. Fülöp (Trieste: PoS), 145
Doherty C. L., Gil-Pons P., Siess L., Lattanzio J. C., Lau H. H. B. 2015, MNRAS, 446, 2599
Fujimoto M. Y., Iben Jr. I., Hollowell D. 1990, ApJ, 349, 580
Gallino R., Arlandini C., Busso M., Lugaro M., Travaglio C., Straniero O., Chieffi A., Limongi M. 1998, ApJ, 497, 388
Goswami A., Aoki W. 2010, MNRAS, 404, 253
Goswami A., Aoki W., Beers T. C., *et al*. 2006, MNRAS, 372, 343
Goswami A., Athiray S. P., Karinkuzhi D. 2010, Astrophysics and Space Science Proceedings, 17, 211
Hampel M., Karakas A. I., Stancliffe R. J., Meyer B. S., Lugaro M. 2019, ApJ, 887, 11
Hampel M., Stancliffe R. J., Lugaro M., Meyer B. S. 2016, ApJ, 831, 171
Hansen C. J., Hansen T. T., Koch A., *et al*. 2019, A&A, 623, A128
Hill V., Barbuy B., Spite M., *et al*. 2000, A&A, 353, 557
Iben Jr. I., Renzini A. 1983, ARA&A, 21, 271
Ivans I. I., Sneden C., Gallino R., Cowan J. J., Preston G. W. 2005, ApJ, 627, L145
Jones S., Ritter C., Herwig F., *et al*. 2016, MNRAS, 455, 3848
Jonsell K., Barklem P. S., Gustafsson B., *et al*. 2006, A&A, 451, 651
Lau H. H. B., Stancliffe R. J., Tout C. A. 2008, MNRAS, 385, 301
Lucatello S., Gratton R. G., Beers T. C., Carretta E. 2005, ApJ, 625, 833
Lugaro M., Campbell S. W., de Mink S. E. 2009, PASA, 26, 322
Matrozis E., Stancliffe R. J. 2016, A&A, 592, A29
Nomoto K., Sugimoto D., Neo S. 1976, Ap&SS, 39, L37
Purandardas M., Goswami A., Goswami P. P., Shejeelammal J., Masseron T. 2019, MNRAS, 486, 3266
Qian Y. Z., Wasserburg G. J. 2003, ApJ, 588, 1099
Qian Y. Z., Woosley S. E. 1996, ApJ, 471, 331
Richard O., Michaud G., Richer J., *et al*. 2002, ApJ, 568, 979
Stancliffe R. J., Dearborn D. S. P., Lattanzio J. C., Heap S. A., Campbell S. W. 2011, ApJ, 742, 121
Thielemann F.-K., Arcones A., Kappeli R., *et al*. 2011, PrPNP, 66, 346
Tsuji T., Tomioka K., Sato H., Iye M., Okada T. 1991, A&A, 252, L1
Wehmeyer B., Pignatari M., Thielemann F.-K. 2015, MNRAS, 452, 1970
Zijlstra A. A. 2004, MNRAS, 348, L23